JOURNAL OF SOLID STATE CHEMISTRY 51, 104–117 (1984)

Neutron and X-Ray Powder Diffraction Study of Li_xRuO_2 and Li_xIrO_2: The Crystal Structure of $Li_{0.9}RuO_2$

ISOBEL J. DAVIDSON* AND J. E. GREEDAN

Institute for Materials Research and Chemistry Department, McMaster University, Hamilton, Ontario L8S 4M1, Canada

Received June 21, 1983, and in final form August 17, 1983

Compounds formed by the insertion of lithium into the rutile structure hosts RuO_2 and IrO_2 were studied by X-ray and neutron powder diffraction techniques. Compositions in the range Li_xMO_2, M = Ru or Ir, $0 < x < 1$ are two-phase materials consisting of unreacted host, $x = 0$, and limiting compositions $x = 0.9$ in both cases. Preparation of compounds with $x > 1$ was unsuccessful. $Li_{0.9}RuO_2$ and $Li_{0.9}IrO_2$ have orthorhombic cells with $a = 5.062(3)$, $b = 4.967(4)$, $c = 2.771(4)$ and $a = 4.962(4)$, $b = 4.758(4)$, $c = 3.108(6)$, respectively. Compared to the host rutile (tetragonal) cells those of the insertion compounds are greatly expanded along [100] and [010], ~0.5 Å for both, and contracted along [001], by ~0.3 Å for $Li_{0.9}RuO_2$ and 0.05 Å for $Li_{0.9}IrO_2$. The space group for both insertion phases appears to be $Pnnm$, a subgroup of the rutile space group $P4_2/mnm$. The structure of $Li_{0.9}RuO_2$ was solved from neutron diffraction data. Lithium exists as Li^+ in octahedral sites. The Li–O coordination is highly regular with two bonds at 2.05(1) Å and four at 2.08(2) Å. The overall structure is essentially an ordered NiAs-type very similar to but more regular than the previously reported $LiMoO_2$. Attempts to solve the structure of $Li_{0.9}IrO_2$ from both X-ray and neutron powder data were unsuccessful due, presumably, to severe preferred orientation.

Introduction

Chemical systems involving the introduction or insertion of guest species into the crystal lattice of a host have received renewed attention recently. The most familiar systems involve layer-structure hosts such as graphite or transition metal dichalcogenides and electron donating guest species, i.e., Lewis bases, especially the electropositive metals. Due to technological interest in solid state batteries, lithium insertion compounds have attracted particular attention. Quite recently, the class of host materials has been expanded to include those with network structures having vacant channels with sites large enough to accommodate the lithium guests. A number of these network hosts are transition metal oxides with relatively simple structures.

A recent report indicates that certain oxides with the tetragonal rutile structure, MO_2, M = Cr, Ru, Os, Ir, can accept rather large amounts of lithium. Stoichiometries such as $Li_{1.3}RuO_2$ and $Li_{1.5}IrO_2$ have been claimed (*1*). No X-ray data were reported, but a set of "pseudo-tetragonal" lattice constants were given for the lithium insertion phases which indicated a cell volume expansion of 10 to 20% compared to the rutile host. In the case of RuO_2, for example, the pseudo-tetragonal a axis expands from 4.49 to 5.04 Å while the c axis actually

* Current address: Ballard Research Inc., 1164 West 15th Street, North Vancouver, British Columbia V7P 1M9, Canada

0022-4596/84 $3.00

contracts from 3.11 to 2.78 Å. From the apparent similarity of the powder patterns of the lithiated and host rutile phases and the relative ease of interconversion between the two it was argued that a close structural relationship must exist. It was therefore proposed that the most likely sites for the lithium atoms are octahedral and/or tetrahedral sites available in the vacant channels parallel to the [001] direction in the host rutile lattice.

Baur has also considered the possible structure of these lithium insertion phases (*2*). He has noted that the reported *c*/*a* ratios correspond closely to the ideal ratio for tetragonal close packing, an arrangement actually found for several complex lithium oxides, such as Li_4GeO_4, in which all of the cations are tetrahedrally coordinated. Baur therefore suggests that some or all of the lithium atoms may be on tetrahedral sites.

It is obvious that a detailed structural study of these interesting materials would be useful not only to provide basic crystal chemical data but also as a guide to an eventual understanding of their physical properties. When the study described here was begun there existed no published reports regarding the structure of any of these phases. Since then the structure of $LiMoO_2$ has been solved (*3*). Here the host material, MoO_2, has a monoclinic structure related to rutile. The lithium ions were found to occupy octahedral sites with Li–O bond lengths ranging from 2.04 to 2.18 Å.

As these materials are available only as rather air-sensitive powders and given that Li^+ is difficult to detect by X-ray methods we have attempted to determine the structures of Li_xRuO_2 and Li_xIrO_2 from powder neutron diffraction data.

Experimental

Preparation of RuO_2 and IrO_2

Polycrystalline RuO_2 was prepared by heating amorphous RuO_2 (Atomergic Chemical Co.) in air in a platinum crucible to 900°C for a minimum of 15 hr. Crystals of IrO_2 were initially prepared by the gas transport reaction of Rogers *et al.* (*4*), which involves the oxidation of Ir sponge in a stream of dry O_2 at 1000°C and the subsequent transport of IrO_2 via the higher oxide, IrO_3.

The iridium sponge (7 g from Johnson-Matthey Ltd.) was placed into two alumina boats, which were then loaded into a silica tube. The tube was then inserted into a horizontal tube furnace. The oxygen flow was set at 17 ml/min and the furnace was heated to 1000°C for 24 hr to oxidize the iridium metal. The temperature of the charge was then raised to 1190°C for 2 weeks. Unfortunately, only about 8% of the charge was transported in the form of purplish-black polyhedral chunks and flat plates of IrO_2. The material left in the alumina boats was a very hard, greyish-black mass of partially oxidized Ir metal, even though the boats had been initially loaded with finely ground powder. This suggested that the Ir metal sintered together before it could all be oxidized, making oxygen diffusion difficult.

More complete reaction was obtained by exposing the Ir/IrO_2 mixture to a higher pressure of O_2. This was accomplished by sealing the Ir/IrO_2 mixture in a quartz tube with a chemical source of oxygen, $NaClO_3$, and heating it to 1190°C for 2 days in an induction heated furnace.

Pressures of up to 4 atm (at 1190°C) were supported by the quartz tube by pressurizing the furnace chamber to about 2 atm with argon. The IrO_2 transported in this way was deposted as fine needles. The crystals of IrO_2 were then ground finely.

Preparation of Li_xRuO_2 and Li_xIrO_2

The lithium intercalates of RuO_2 and IrO_2 were formed on exposure at ambient temperature of the host rutile type MO_2 to a 0.2 *M* solution of *n*-butyl lithium (Aldrich Chemical Co.) in hexane (*5*) under argon in

a glove box. After 1 to 2 weeks of reaction, the hexane solution was decanted and the material was then rinsed twice with about 25 ml of hexane and dried under vacuum for about 2 hr. Samples with smaller nominal lithium compositions ($x \approx 0.2$, for example) were prepared by decreasing the quantity of *n*-butyl lithium used. In these preparations about half of the lithium present in the solution was incorporated in the product. For RuO_2 the largest x values ($x \approx 0.9$) were obtained with a 1.5 to 1.9 molar excess of lithium at a concentration of 0.20 to 0.24 *M* and a reaction duration of 8 to 12 days. In the case of IrO_2, a nominal composition of $Li_{0.87}IrO_2$ was produced from a 13-day reaction with a 3.2 molar excess of lithium at a concentration of 0.34 *M*. Attempts to prepare samples with a large lithium content, that is, $x \geq 1$, by increasing the molar excess and concentration of lithium in solution generally had the effect of lowering the quantity of lithium inserted. Similarly, increasing the duration of the reaction beyond 1 week had no dramatic effect on the lithium composition of the product. However, a systematic study of the effects of these and other parameters on lithium uptake is required before any conclusive comments can be made.

Lithium Analysis

The lithium content of the intercalation products was initially determined by titration of the initial and residual reagent, as described by Dines (*5*) and by atomic absorption. Since the titration method of (*5*) gave a much higher lithium assay than by atomic absorption, a third analysis technique involving the direct titration of the water-decomposed intercalation product was employed. Li_2CO_3 was used as the standard for the analyses by atomic absorption.

X-ray Diffraction

The lattice parameters of the intercalated materials were determined from X-ray powder diffraction data collected on a Philips diffractometer with monochromatized Cu$K\alpha$ radiation using KCl as an internal standard. Data were collected over the range of about $5° \leq 2\Theta \leq 80°$ with a scan rate of 1/2°/min. Generally about 9 or 10 well-resolved peaks were obtained, from which the lattice parameters were determined by least squares refinement.

The intercalation products, Li_xMO_2 (M = Ru, Os, and Ir), decompose very rapidly on exposure to air or moisture and consequently must be protected while the X-ray diffraction pattern is obtained. The samples were prepared in an argon-filled dry box by pressing finely ground powder into a vertical groove in a glass slide, and covering with a double layer of plastic wrap held with transparent tape. The plastic wrap window produced a broad peak around 21.5° in 2Θ, which did not overlap any sample peaks.

Neutron Diffraction

Neutron diffraction data were collected on the triple axis spectrometer (in double axis mode) at McMaster University Research Reactor. The data were collected at neutron wavelength of 1.40 Å obtained from the (200) reflection of a single crystal of copper. Instrumental parameters such as the zero angle, precise wavelength, and resolution were determined from the diffraction pattern of finely divided polycrystalline copper. The spectrometer is equipped with a position sensitive detector (PSD), which consists of two linear ^3He detector tubes, 2.54 cm diam. × 61 cm long, mounted horizontally one above the other. In its present configuration the angular range scanned for a given detector position is 35°(2θ) which is subdivided into 256 channels, i.e., data points are collected at 0.137°(2θ) intervals. The data are corrected for parallax and other geometrical effects due to the linear tube configuration. The air-sensitive sam-

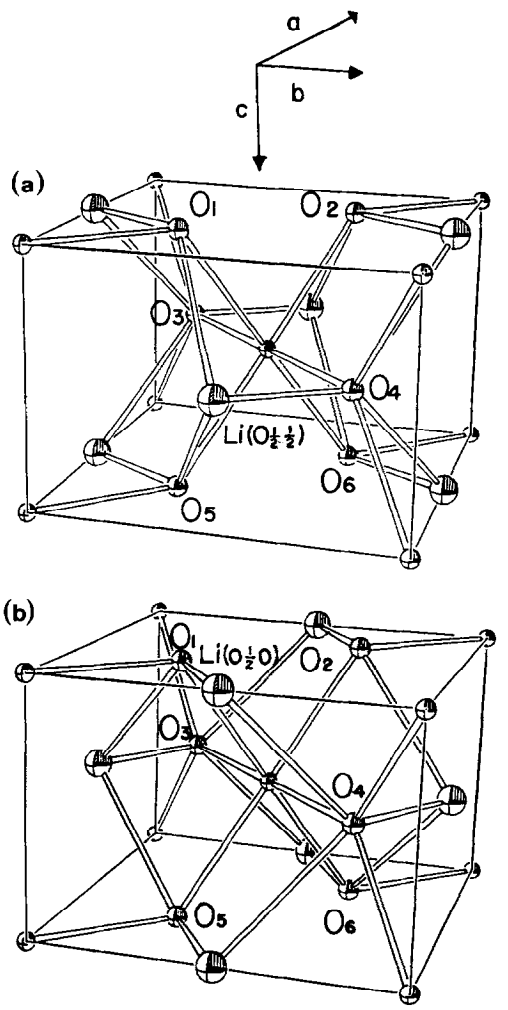

FIG. 1. Possible octahedral (six-fold) sites for lithium within the rutile host cell. These are the 4c sites. 1(a) shows the pair $\frac{1}{2},0,0$ and $0,\frac{1}{2},\frac{1}{2}$. 1(b) the pair $0,\frac{1}{2},0$ and $\frac{1}{2},0,\frac{1}{2}$.

ples were contained in argon-filled, thin-walled, vanadium cylinders of 4 or 8 mm diameter which were sealed with a flat Teflon gasket.

Structural Models

The Host Structure

We begin by assuming that the structure of the lithium insertion phases is similar to that of the rutile host, MO_2. The M atoms are in positions $2a$, 000, and $\frac{1}{2}\frac{1}{2}\frac{1}{2}$, while the O atoms are in $4f$, $x,x,0$; $\bar{x},\bar{x},0$; $\frac{1}{2}+x, \frac{1}{2}-x, \frac{1}{2}$; $\frac{1}{2}-x, \frac{1}{2}+x, \frac{1}{2}$ of spacegroup $P4_2/mnm$ (No. 136). The vacant channel sites suggested by Murphy *et al.* (*1*) for the lithium atoms are octahedral sites ($4c$)—$0,\frac{1}{2},0$; $\frac{1}{2},0,\frac{1}{2}$; $0,\frac{1}{2},\frac{1}{2}$; $\frac{1}{2},0,0$; and tetrahedral sites ($4d$)—$0,\frac{1}{2},\frac{1}{4}$; $0,\frac{1}{2},\frac{3}{4}$; $\frac{1}{2},0,\frac{1}{4}$; $\frac{1}{2},0,\frac{3}{4}$. Figure 1 shows the octahedral sites and Fig. 2 the tetrahedral sites in the undistorted host cell. For the expected $Li/M \simeq 1$ note that both types of site are likely to be occupied in pairwise fashion to minimize Li^+–Li^+ repulsions, i.e., either $\frac{1}{2},0,0$ and $0,\frac{1}{2},\frac{1}{2}$ or $0,\frac{1}{2},0$ and $\frac{1}{2},0,\frac{1}{2}$ for the six-fold sites and $\frac{1}{2},0,\frac{1}{4}$ and $0,\frac{1}{2},\frac{3}{4}$ or $0,\frac{1}{2},\frac{1}{4}$ and $\frac{1}{2},0,\frac{3}{4}$ for the fourfold sites. In the undistorted host, there would be four long and two short bonds for the octahedral site

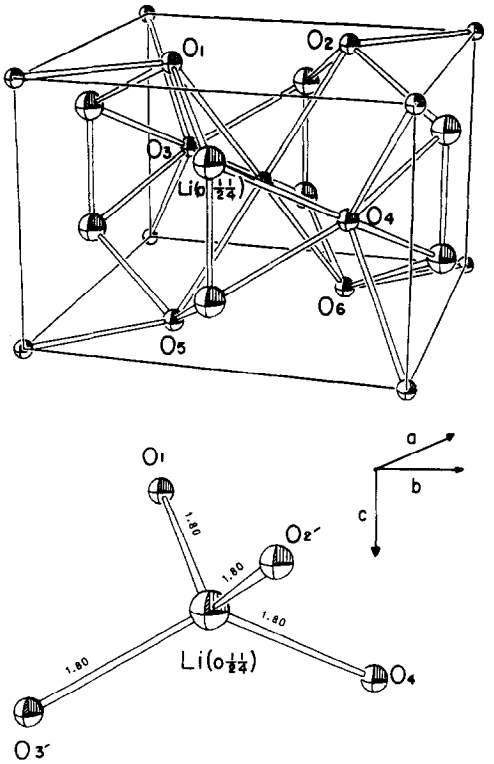

FIG. 2. Possible tetrahedral (four-fold) sites for lithium within the rutile host cell. These are the 4d sites.

TABLE I

LATTICE CONSTANTS FOR THE ORTHORHOMBIC PHASE IN MATERIALS OF COMPOSITION Li_xRuO_2

$x \pm 0.5$	a (Å)	b (Å)	c (Å)	Vol. (Å^3)
0.0	4.4930(20)		3.1050(20)	62.68(10)
0.15[a]	5.066	4.966	2.776	
0.26[a]	5.066	4.966	2.776	
0.52	5.0588(40)	4.9614(42)	2.7789(24)	69.75(17)
0.54	5.0700(41)	4.9696(43)	2.7751(27)	69.93(19)
0.86	5.0618(31)	4.9667(36)	2.7713(35)	69.67(18)
0.87	5.0729(31)	4.9662(29)	2.7809(37)	70.06(18)
Ave.	5.066(36)	4.966(38)	2.776(31)	

[a] Too few peaks from the orthorhombic phase were present in these lower compositions to fit the cell parameters, but the observed peaks are reasonably well-described (±0.08°) by the average cell parameters.

Note. Values in parentheses are estimated standard deviations referring to the least significant digit(s).

TABLE II

LATTICE CONSTANTS FOR THE ORTHORHOMBIC PHASE IN MATERIALS OF COMPOSITION Li_xIrO_2

$x \pm 0.05$	a (Å)	b (Å)	c (Å)	Vol. (Å^3)
0.0	4.4987(13)		3.1552(27)	63.86(9)
0.28	4.9678(36)	4.7573(41)	3.1034(38)	73.34(21)
0.37	4.9607(28)	4.7592(26)	3.0975(51)	73.13(20)
0.64	4.9701(42)	4.7591(38)	3.1074(45)	73.50(23)
0.87	4.9615(41)	4.7579(36)	3.1084(59)	73.38(26)
0.88	4.9688(39)	4.7573(38)	3.1063(54)	73.43(24)

Note. Values in parentheses are estimated standard deviations referring to the least significant digit(s).

(2.25 and 1.63 Å, respectively, in RuO_2) while the four-coordinated sites would have four equal bond lengths (1.80 Å in RuO_2). Since the crystal radius of Li+ is 0.90 Å for six-coordination and 0.73 Å for four-coordination, while that of oxygen is 1.26 Å (*6*), some distortion of the host cell on lithium insertion is to be expected. It is also valuable to note that the expected pairwise occupation of either the octahedral (4*c*) or tetrahedral (4*d*) sites requires that the insertion product belong to a crystal class with less than tetragonal symmetry.

X-ray Powder Data for Li_xRuO_2 and Li_xIrO_2

X-ray powder data were collected for several compositions in the range $0.2 < x < 0.9$ for both Li_xRuO_2 and Li_xIrO_2. For all compositions studied with $x < 0.9$ two phases were observed, with one phase being the host MO_2. For $x \approx 0.9$ we found only one phase by X-rays. This is essentially the same behavior reported by Murphy *et al.* (*1*) but our limiting composition is much smaller than $x = 1.3$ reported by them. We were unsuccessful in all attempts to prepare insertion phases with $x > 1$. The powder data for both $Li_{0.9}RuO_2$ and $Li_{0.9}IrO_2$ could be indexed on an orthorhombic cell with the lattice constants shown in Tables I and II. Indexed powder data for $Li_{0.87}RuO_2$ and $Li_{0.87}IrO_2$ are given in Table III.

TABLE III

INDEXED d SPACINGS FOR $Li_{0.87}RuO_2$ AND $Li_{0.87}IrO_2$

$Li_{0.87}RuO_2$			$Li_{0.87}IrO_2$		
hkl	d (Å)	I/I_o	*hkl*	d (Å)	I/I_o[a]
110	3.557	100	110	3.444	—
200	2.537	12	101	2.635	—
020	2.486	20	011	2.606	—
101, 011	2.431	50	200	2.487	—
210, 120	2.226	10	020	2.384	—
111	2.189	4	211	1.799	—
220	1.776	25	121	1.768	—
211	1.752	30	220	1.721	—
121	1.741	20	310, 002	1.567	—
310	1.602	10	130, 221	1.513	—
130	1.573	5	301	1.464	—
301	1.445	5	112	1.415	—
031	1.424	10	202	1.317	—
320, 002, 230, 311, 131	1.390	5	022	1.301	—
			321, 400	1.245	—
			231	1.230	—
112	1.294	5			
400	1.270	5			

[a] Relative intensities were not reproducible.

TABLE IV

CORRESPONDING POSITIONS IN $P4_2/mnm$ AND $Pnnm$

$P4_2/mnm$		$Pnnm$	
2*a*	0,0,0, $\frac{1}{2},\frac{1}{2},\frac{1}{2}$;	2*a*	0,0,0; $\frac{1}{2},\frac{1}{2},\frac{1}{2}$
4*c*	$0,\frac{1}{2},0$; $\frac{1}{2},0,0$; $0,\frac{1}{2},\frac{1}{2}$; $\frac{1}{2},0,\frac{1}{2}$	2*c*	$0,\frac{1}{2},0$; $\frac{1}{2},0,\frac{1}{2}$
		2*d*	$0,\frac{1}{2},\frac{1}{2}$; $\frac{1}{2},0,0$
4*d*	$0,\frac{1}{2},\frac{1}{4}$; $\frac{1}{2},0,\frac{1}{4}$; $0,\frac{1}{2},\frac{3}{4}$; $\frac{1}{2},0,\frac{3}{4}$;	4*f*	$0,\frac{1}{2},z$; $0,\frac{1}{2},\bar{z}$; $\frac{1}{2},0,\frac{1}{2}-z$; $\frac{1}{2},0,\frac{1}{2}+z$
4*f*	$x,x,0$; $\bar{x},\bar{x},0$; $\frac{1}{2}+x,\frac{1}{2}-x,\frac{1}{2}$; $\frac{1}{2}-x,\frac{1}{2}+x,\frac{1}{2}$	4*g*	$x,y,0$; $\bar{x},\bar{y},0$; $\frac{1}{2}+x,\frac{1}{2}-y,\frac{1}{2}$; $\frac{1}{2}-x,\frac{1}{2}+y,\frac{1}{2}$

Using the approach of Visser (*7*) a search was made for other cells which might also fit the observed powder data but it was found in all cases that the orthorhombic cell provided the best fit. Note that the orthorhombic cell dimensions indicate an expansion of about 0.5 Å along the [100] and [010] directions relative to the host cells of RuO_2 and IrO_2 and a contraction along [001] of about 0.3 Å for RuO_2 and 0.05 Å for IrO_2. This leads to a cell volume expansion of 12% for $Li_{0.9}RuO_2$ and 15% for $Li_{0.9}IrO_2$ relative to the host cells. These are somewhat smaller than the cell expansions reported in (*1*) but it is impossible to determine if this is significant due to the different indexing schemes used and the fact that no errors were assigned to the cell constants of (*1*).

Space Group

Assuming the orthorhombic cell described above the following sets of systematic absences were observed: $(0kl)$ $k + l = 2n + 1$, $(h0l)$ $h + l = 2n + 1$, $(h00)$ $h = 2n + 1$, $(0k0)$ $k = 2n + 1$, $(00l)$ $l = 2n + 1$. These are consistent with only two orthorhombic space groups: *Pnnm* (no. 58) and *Pnn*2 (no. 34), its noncentrosymmetric counterpart. The centrosymmetric group was chosen for the initial refinement.

We note that *Pnnm* is a subgroup of $P4_2/mnm$ obtained by removal of the 4_2 axis. Consequently, corresponding sites are found in the two groups as shown in Table IV. Trial sites for the atoms in $Li_{0.9}RuO_2$ or $Li_{0.9}IrO_2$ in *Pnnm* are, therefore, Ru/Ir in 2*a*, O in 4*g*, and Li in either 2*c*, 2*d*, or partially occupying 4*f*.

Structure Refinement of $Li_{0.9}RuO_2$ from X-ray and Neutron Powder Data

A check on the trial positions for the heavy atoms and oxygen can in principle be obtained from X-ray powder data. A total of 15 integrated intensities for $Li_{0.87}RuO_2$ were used for such a preliminary refinement. A suitable X-ray data set could not be obtained for any sample of Li_xIrO_2. The needlelike habit of the IrO_2 host crystals and the flat plate geometry used for the powder samples would tend to aggravate preferred orientation.

Table V, column one, shows the results of the refinement of the $Li_{0.87}RuO_2$ X-ray data. The agreement indices of $R = 8\%$, $R_w = 9\%$ indicate that the trial positions for Ru and O are not unreasonable. The negative temperature factors are probably indicative of some degree of preferred orientation and/or that the lithium electron density has not been included.

Powder neutron data sets were collected at room temperature for two samples of Li_xRuO_2 of nominal compositions $x = 0.86(5)$ and $0.87(5)$ over the 2θ range from 4 to 90° by moving the PSD about the diffraction circle. Data were collected at five fixed po-

TABLE V

STRUCTURAL PARAMETERS FROM REFINEMENT OF POWDER DATA FOR $Li_{0.9}RuO_2$

		$Li_{0.87}RuO_2$		$Li_{0.86}RuO_2$
		X-ray 1.54 Å	Neutron 1.40 Å	Neutron 1.40 Å
Ru	*X*	0.0	0.0	0.0
	Y	0.0	0.0	0.0
	Z	0.0	0.0	0.0
	B (Å^2)	−0.10(29)	0.31(35)	0.95(22)
O	*X*	0.240(13)	0.2555(40)	0.2501(26)
	Y	0.356(35)	0.3365(44)	0.3316(35)
	Z	0.0	0.0	0.0
	B (Å^2)	−1.3(2.0)	0.09(26)	0.37(15)
Li	*X*	—	0.0	0.0
	Y	—	0.5	0.5
	Z	—	0.5	0.5
	B (Å^2)	—	2.7(2.0)	0.32(76)
R		7.6	9.62	8.13
R_w		9.18	10.24	7.22
No. of *I*		15	21	21
No. of *hkl*		36	58	73

Note. Neutron scattering lengths taken as −0.203, 0.73, and 5.8 × 10^{-12} cm for Li, Ru, and O, respectively (*15*). Values in parentheses are estimated standard deviations referring to the least significant digit(s).

sitions chosen to overlap by 10°(2θ) each. The datasets were corrected for effects due to the linear tube geometry and were scaled appropriately. The data for $Li_{0.87}RuO_2$ are shown in Fig. 3. No reflections were observed in the 4 to 20°(2θ) range.

To refine the structure we have chosen to use integrated intensities rather than the total diffraction profile and a fitting approach such as that described by Rietveld (*8*). This choice was dictated by the relatively low resolution of our diffractometer, especially at higher angles, and the smaller number of profile data points available as compared to data obtained on high-resolution facilities. However, we have used a profile fitting method to extract integrated intensities from regions of the powder pattern containing overlapping but partially resolved reflections. We attempt to deconvolute or fit only those regions of the diffraction profile which exhibit fairly well-resolved intensity maxima which can be assigned to a small number of single reflections or bunched groups of reflections which may be treated as single Gaussians. The appropriate variances are taken from data on Cu powder obtained in the same sample holders. The background is fitted to a linear function and the profile is fitted to a set of overlapping Gaussians using a nonlinear least squares method. Examples of the fitting procedure and the fits obtained are illustrated for the regions 35–40°(2θ) and 65–70°(2θ) in Figs. 4a and b. For the range 35 to 40°, Fig. 4a, there are only two reflections which contribute to the profile and the fit is seen to be good. Six reflections, Fig. 4b, contribute to the profile from 65 to 70° but the two intensity maxima at lower angles correspond to single reflections while the third at higher angles is comprised of four reflections. To treat this situation we fix the variances of the first two Gaussians at the appropriate values and fit the variance of the third. The overall fit here is not as good as in Fig. 4a but is still satisfactory given the quality of the dataset. A second method was used to determine the group intensity of the four reflections associated with the high angle maximum in Fig. 4b. This intensity is equal to the total integrated intensity for this part of the profile minus the sum of the two single reflection intensities at lower angles. The group intensities determined by the two methods agree within one standard error. For other regions of the diffraction profile such as that between 45 and 50°(2θ) in which three reflections are associated with a single peak with no resolved features, the group intensity is extracted by straightforward integration. Using the procedures outlined and illustrated above 21 separate intensities were extracted from each dataset and used in the structure refinement. The observed and calculated intensities are shown in Table VI.

As a check on the data collection, handling, and refinement procedure, the structure of the pure host material RuO_2 was refined and compared to the results of a single

crystal determination (*9*). The agreement, Table VII, between the oxygen parameter obtained by the two methods is seen to be good.

As mentioned the most probable sites for lithium atoms in $Li_{0.9}RuO_2$ are the channel sites 2*c*, 2*d*, or 4*f*. Refinements of the structures for both preparations of nominal composition $Li_{0.9}RuO_2$ were attempted with all of the lithium in each of these three sites and with the lithium distributed in various ratios over all possible combinations of two of the three sites. The best fits to the observed intensities were obtained with all of the lithium in 2*d* or in approximately half of the 4*f* sites. In the case of the 4*f* site ($0\frac{1}{2}z$) the *z* parameter refined to 0.48(7), and therefore this site is six-coordinated and in fact the result is identical with the 2*d* site model. Furthermore, the weighted agreement factors differ only slightly, $R_w = 7.22$ for 2*d* and 7.21 for 4*f* in the case of

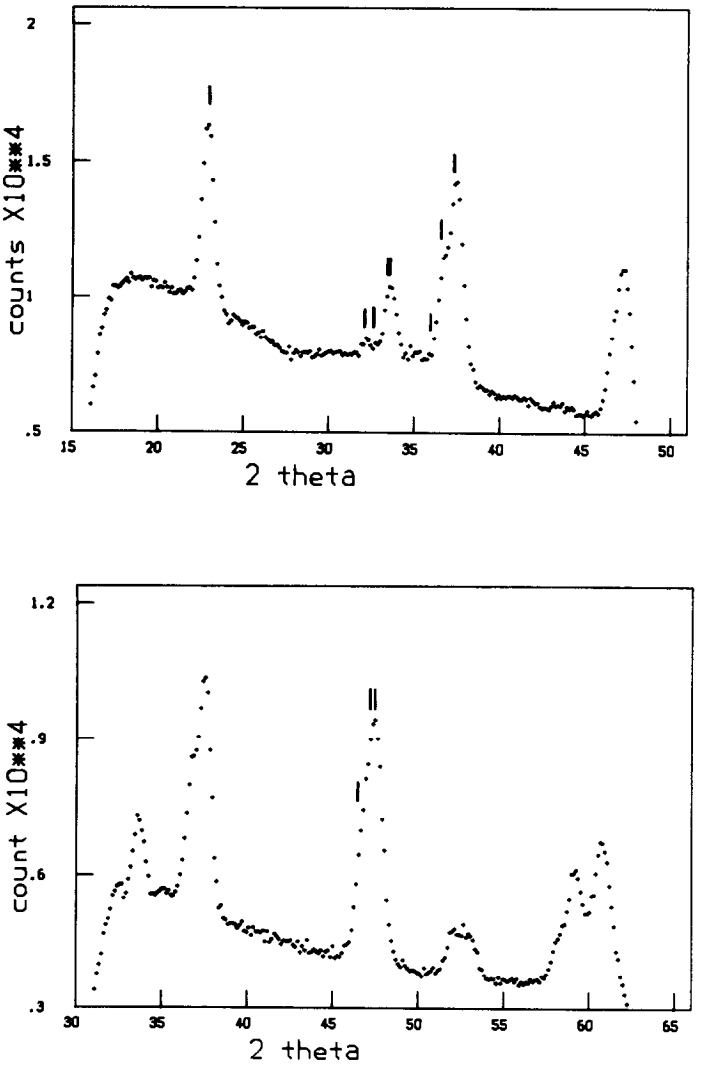

FIG. 3. Neutron diffraction data for $Li_{0.87}RuO_2$. The positions of Bragg reflections are indicated.

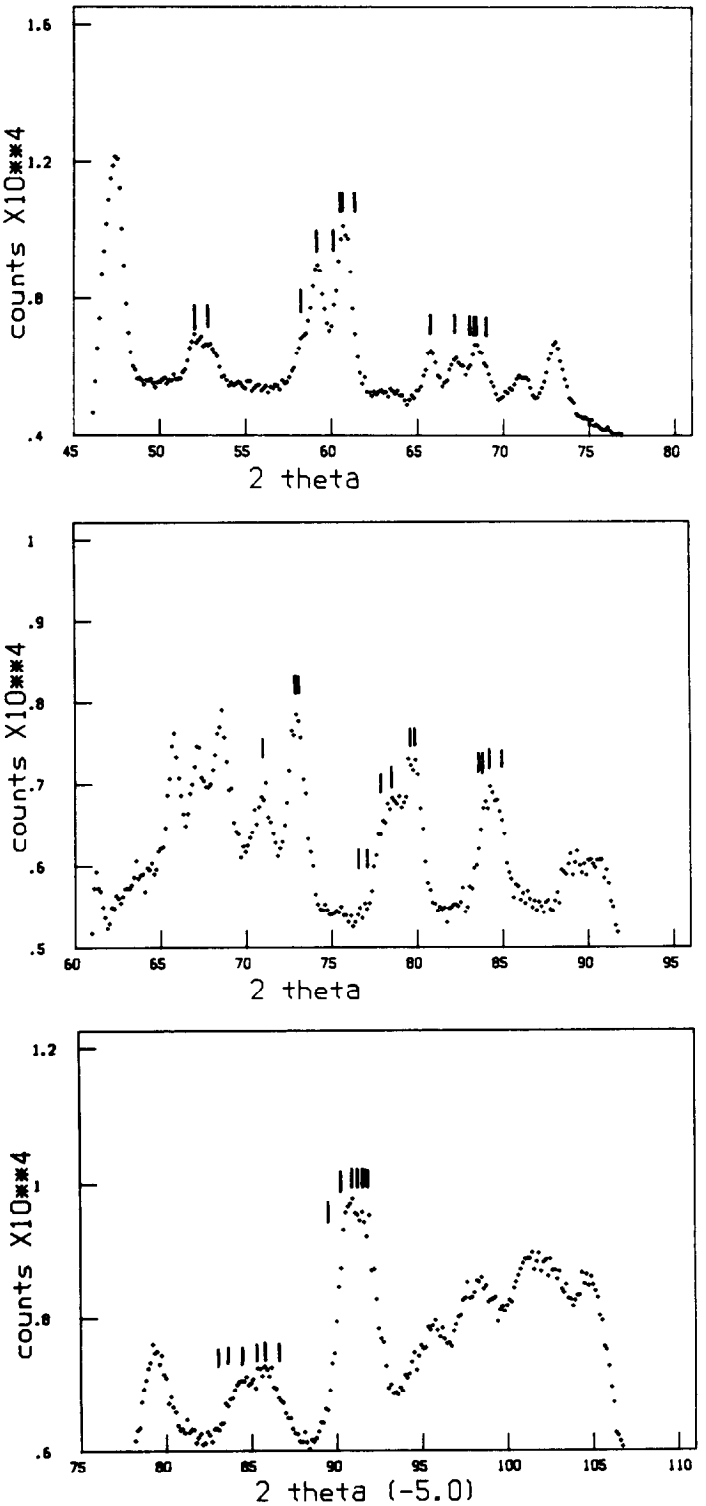

FIG. 3—*Continued.*

TABLE VI

OBSERVED AND CALCULATED INTENSITIES FOR $Li_{0.86}RuO_2$ AND $Li_{0.87}RuO_2$

$Li_{0.87}RuO_2$					$Li_{0.86}RuO_2$				
h	*k*	*l*	I_o	I_c	*h*	*k*	*l*	I_o	I_c
1	1	0	6178.39	6481.19	1	1	0	24159.00	25845.30
2	0	0		624.05	2	0	0		3179.38
0	2	0		3.49	0	2	0		32.14
1	0	1		2647.07				3854.60	3211.52
0	1	1		.77	1	0	1		11957.11
			2535.41	3275.38	0	1	1		15.28
2	1	0		13.97				10670.60	11972.39
1	2	0		3048.68	2	1	0		.02
			3026.98	3062.65	1	2	0		12621.38
1	1	1	5857.59	5483.15	1	1	1		25170.15
2	2	0		2376.55				41332.00	37791.55
2	1	1		5144.71	2	2	0		10355.53
1	2	1		3028.58	2	1	1		18995.42
			10028.75	10549.85	1	2	1		11982.73
3	1	0	1103.78	1067.58				41993.00	41333.68
1	3	0	1117.65	1085.01	3	1	0	4790.00	5016.03
2	2	1	1.00	12.60	1	3	0	5058.40	4863.79
3	0	1		1272.47	2	2	1	1.00	.02
0	3	1		3653.31	3	0	1		4076.54
			4414.51	4925.78	0	3	1		14904.44
3	2	0	1154.49	1130.88				18404.40	18980.98
0	0	2		1752.38	3	2	0		5122.99
3	1	1		2081.22	2	3	0		.00
2	3	0		.02	0	0	2		7092.22
1	3	1		9.93	3	1	1		10482.64
			4444.99	3843.56	1	3	1		14.42
1	1	2	1198.96	1672.93				20986.90	22712.27
4	0	0	1036.10	1453.19	1	1	2	5492.20	6451.52
3	2	1		1318.43	4	0	0	5428.60	5936.89
0	4	0		.08	3	2	1		5982.24
2	3	1		393.65	0	4	0		4.70
4	1	0		15.43	2	3	1		3781.50
			1602.03	1727.59				10611.10	9768.44
2	0	2		188.12	4	1	0	958.90	.03
0	2	2		15.13	2	0	2		1844.32
1	4	0		722.44	0	2	2		54.76
			1477.24	925.69	1	4	0		4235.50
2	1	2		7.17				4233.50	6134.59
3	3	0		853.47	3	3	0		2701.69
1	2	2		1594.42	2	1	2		.01
			2634.91	2455.06	1	2	2		7544.08
4	2	0		17.89				9835.00	10245.78
4	1	1		14.39	4	2	0		57.29
2	4	0		1235.67	4	1	1		63.60
1	4	1		1241.43	2	4	0		3563.39
			2170.69	2509.38	1	4	1		4703.03
2	2	2		1998.38				8037.60	8387.32
3	3	1		6.06	2	2	2		7771.09
			1659.60	2004.44	3	3	1		9.65
3	1	2		941.15				7689.40	7780.74
4	2	1		23.64	3	1	2		4207.31
1	3	2		975.87	4	2	1		.04
2	4	1		5.03	1	3	2		4157.87
			2243.82	1945.69	2	4	1		.01
4	3	0		.05				7799.00	8365.23
3	4	0		488.01	4	3	0		.00
5	1	0		602.49	3	4	0		3134.69
			1110.47	1090.55	5	1	0		1914.07
3	2	2		1095.32	3	2	2		5689.93

TABLE VI—*Continued*

$Li_{0.87}RuO_2$					$Li_{0.86}RuO_2$				
h	*k*	*l*	I_o	I_c	*h*	*k*	*l*	I_o	I_c
2	3	2		.02	2	3	2		.00
1	5	0		492.64	1	5	0		1847.99
			1516.67	1587.99				10945.50	12586.69
5	0	1		289.92	5	0	1		1751.61
4	3	1		3517.72	4	3	1		14129.87
3	4	1		781.96	3	4	1		3462.55
5	2	0		491.28	5	2	0		2678.36
4	0	2		1738.19	0	5	1		100.58
5	1	1		913.09	4	0	2		6956.00
0	5	1		37.66	5	1	1		5541.28
0	4	2		5.11	2	5	0		.00
2	5	0		2.49	0	4	2		25.08
4	1	2		17.36				33183.00	34645.33
			9570.89	7794.79	1	5	1		5031.80
					4	1	2		.03
					1	4	2		5581.32
					1	0	3		1639.23
					0	1	3		47.23
					3	3	2		3250.82
					1	1	3		5299.65
					5	2	1		3191.46
					4	4	0		29.00
					2	5	1		5750.09
					4	2	2		156.58
					2	4	2		4681.52
					5	3	0		1518.25
					3	5	0		1512.60
					2	1	3		4929.42
					1	2	3		3027.62
								52177.00	45646.62

$Li_{0.86}RuO_2$, and by Hamilton's criterion the 4*f* site with its extra degree of freedom is not significant improvement over the special site at 2*d* (*10*).

The results of the structure refinements for both samples of $Li_{0.9}RuO_2$ are shown in Table V and are seen to agree well with each other and with the X-ray powder refinement.

Attempts to refine the structure of $Li_{0.87}IrO_2$ from similar neutron powder data were unsuccessful. As in the case of the X-ray powder experiments on this material and on the host IrO_2, we suspect that preferred orientation is a problem. We did observe the same sort of orthorhombic cell and the same set of systematic absences for $Li_{0.87}IrO_2$ as for $Li_{0.86}RuO_2$ which strongly suggests the same space group and structure for the two materials.

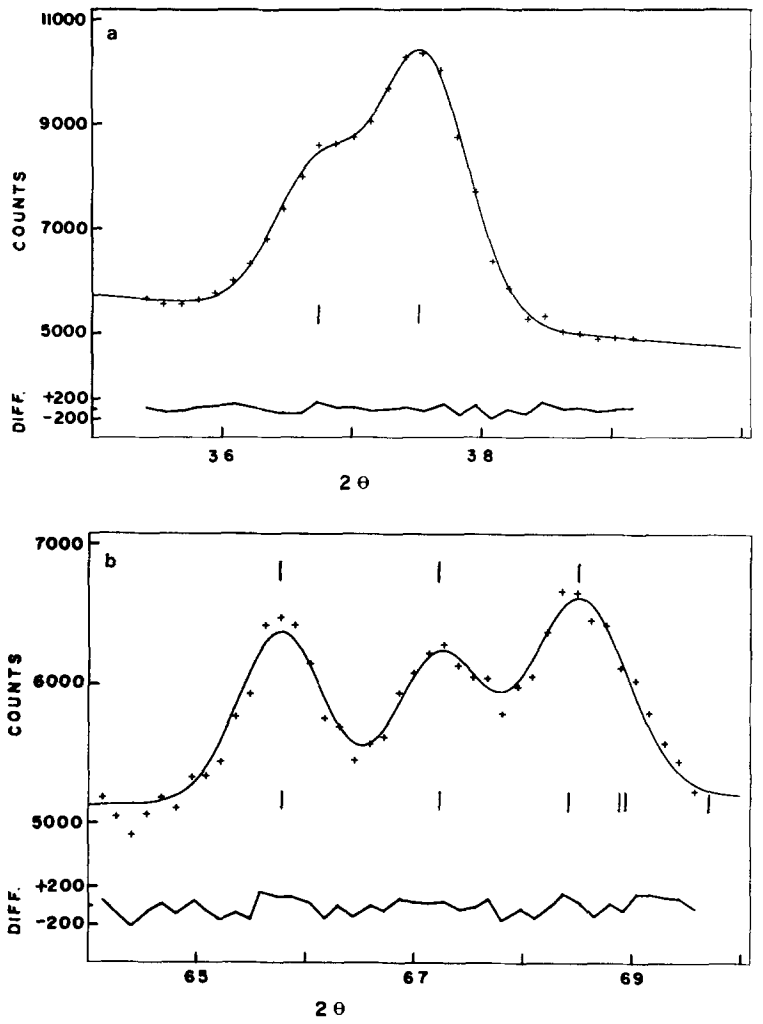

FIG. 4. (a) Fit to the powder diffraction profile of $Li_{0.87}RuO_2$ in the region 35 to 39° (2θ). Positions of the Bragg reflections are indicated below the profile and the difference between the observed and calculated profile points is plotted. (b) Fit to the powder diffraction profile of $Li_{0.87}RuO_2$ in the region 65 to 70° (2θ). Positions of the Bragg reflections are indicated below the profile and the centers of the Gaussians used in the fitting procedure are shown above the profile. The difference between the observed and calculated profile points is plotted.

Discussion of the Structure for $Li_{0.9}RuO_2$

Interatomic distances and angles for $Li_{0.86}RuO_2$, $Li_{0.87}RuO_2$, and RuO_2 are shown in Table VIII. Note that the two Li–O distances are not significantly different. They are also comparable to the Li–O distances found in $LiNbO_3$ (*11*), 2.068(11) and 2.238(23) Å, in $LiReO_3$ (*12*), 2.000(6) and 2.42(1) Å, and $LiMoO_2$ (*3*), 2.04(2) to 2.20(2) Å, in all of which lithium is octahedrally coordinated. Note that the Li–O octahedron is far more regular in $Li_{0.9}RuO_2$ than in any other lithium insertion compound yet investigated. In going from RuO_2 to $Li_{0.9}RuO_2$ the average Ru–O distance increases, consistent with the reduction of

TABLE VII

STRUCTURAL PARAMETERS FROM REFINEMENT OF NEUTRON POWDER DATA FOR RuO_2

		Powder[a] (1.40 Å)	Crystal[b] (Mo$K\alpha$)
Ru	X	0.0	0.0
	Y	0.0	0.0
	Z	0.0	0.0
	B (Å^2)	−0.02(20)	0.384(12)
O	X	0.305(1)	0.3058(16)
	Y	0.305(1)	0.3058(16)
	Z	0.0	0.0
	B (Å^2)	0.22(20)	0.517(8)
	R	5.81	—
	R_w	8.40	—
No. of I		23	—
No. of hkl		27	235

[a] Space group $P4_2/mnm$. Scattering lengths taken as 0.73 and 0.58 × 10^{-12} cm for Ru and O, respectively (*15*). Values in parentheses are estimated standard deviations referring to the least significant digit(s).

[b] Structural parameters obtained from a previous single crystal X-ray study (*9*).

Ru^{IV} to Ru^{III}. In fact the mean Li–O and Ru–O distances are essentially the same in $Li_{0.9}RuO_2$. A corresponding situation is found for $LiMoO_2$ (*3*). This is understandable in terms of the very similar crystal radii reported by Shannon of 0.90, 0.82, and 0.83 Å for Li^+, Ru^{3+}, and Mo^{3+}, respectively (*6*). The shortest Li–Ru distance, not reported in the table, is just $a/2$ = 2.53(2) Å for $Li_{0.86}RuO_2$. This is considerable shorter than the Ru–Ru distance in RuO_2 of 3.105(2) Å or in $Li_{0.86}RuO_2$ of 2.771(4) Å and possibly suggests a strong Li–Ru interaction. An investigation of the electronic structure of these insertion compounds, while difficult from an experimental point of view, might be rewarding.

Although our results show that lithium in Li_xRuO_2, x = 0.9, exists as Li^+ in octahedral coordination, it is worth speculating about the possible structure of similar phases with $x > 1$. $Li_{x>1}MO_2$ represents a case where there are more cations than close packed anions. The cations may be distributed in various ways. For example, if 1.0 lithium atoms occupy the same octahedral sites as in $Li_{0.9}RuO_2$ the additional atoms must enter the $0,\frac{1}{2},z$ sites with $z \sim \frac{1}{4}$. But the crystal radius of four-coordinated Li^+ is 0.73 Å (*6*) while the radius of the $0,\frac{1}{2},\frac{1}{4}$ site is only 0.36 Å assuming no change in cell dimensions. Therefore, we would also expect at the very least a significant expansion in cell dimensions, especially along c, for $x > 1$.

Alternatively we may find a complete change in cation coordination as suggested by Baur (*2*). He points out that a tetragonal close packing of the anions would allow occupation of 1.25 tetrahedral interstices per close packed atom without the energetically unfavorable face sharing between adjacent occupied tetrahedra. An example of such a structure is Li_4GeO_4 in which all cations occupy tetrahedral sites. This structure has a very different symmetry, *Ccmm*, than that found here (*13*).

TABLE VIII

INTERATOMIC DISTANCES AND ANGLES IN RuO_2, $Li_{0.86}RuO_2$, AND $Li_{0.87}RuO_2$ FROM REFINEMENT OF NEUTRON POWDER DATA

	RuO_2	$Li_{0.86}RuO_2$	$Li_{0.87}RuO_2$
	Ru–O octahedron		
Distance	4 at 1.988(3)	4 at 2.054(11)	4 at 2.032(15)
	2 at 1.935(4)	2 at 2.077(16)	2 at 2.115(21)
Angle			
O_1–Ru–O_2	180.0(2)	180.0(7)	180.0(10)
–O_3	102.7(1)	84.8(4)	86.3(6)
–O_4	77.3(1)	95.2(4)	93.7(6)
–O_5	90.0(1)	87.0(5)	86.7(7)
–O_6	90.0(1)	93.0(5)	93.3(7)
O_3–Ru–O_5	90.0(1)	87.0(5)	86.7(7)
	Li–O octahedron		
Distance	—	4 at 2.055(11)	4 at 2.067(15)
	—	2 at 2.077(16)	2 at 2.081(21)
Angle			
$O_{1'}$–Li–$O_{2'}$	—	180.0(7)	180.0(10)
–$O_{3'}$	—	84.8(4)	84.5(5)
–$O_{4'}$	—	95.2(4)	95.5(5)
–$O_{5'}$	—	87.0(5)	86.7(7)
–$O_{6'}$	—	93.0(5)	93.3(7)
$O_{3'}$–Li–$O_{5'}$	—	87.0(5)	86.7(7)

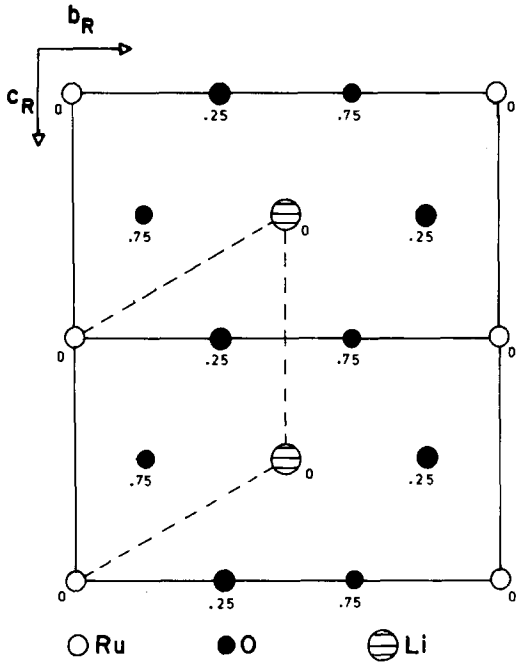

FIG. 5. Projection of the $Li_{0.9}RuO_2$ cell on (100). The rutile-type cell is shown in heavy outline and the NiAs-like cell with broken lines. The numbers give the fractional coordinates along the *a* direction.

Finally, Cox *et al.* (*13*) have pointed out the similarity between the structure of $LiMoO_2$ and the NiAs structure. In fact $Li_{0.9}RuO_2$ is even more closely related to NiAs. Figure 5 shows the relationship between the cell of $Li_{0.9}RuO_2$ and that of a distorted NiAs cell with a_H = 2.844 and 2.771 Å, c_H = 5.062 Å and γ = 119.2°. As discussed by Wells (*14*) the NiAs structure is formed from a hexagonal close packed anion lattice with cations in all octahedral sites. In rutile only one-half the octahedral sites are occupied and the close packed layers distort to give three oxygens coplanar with the nearest cation. For the ideal NiAs cell the cations are at 0,0,0 and 0,0,$\frac{1}{2}$ and the anions at $\frac{1}{3},\frac{2}{3},\frac{3}{4}$ and $\frac{2}{3},\frac{1}{3},\frac{1}{4}$. When transformed to the orthorhombic cell of $Li_{0.86}RuO_2$, the cation sites become the observed positions of Ru and Li at 0,0,0 and 0,$\frac{1}{2},\frac{1}{2}$, respectively, while the anion sites become very close to the observed positions of oxygen at $\frac{1}{4},\frac{1}{3}$,0 and $\frac{3}{4},\frac{1}{6},\frac{1}{2}$ as seen in Table IX.

TABLE IX

COMPARISON OF STRUCTURAL PARAMETERS FROM REFINEMENT OF NEUTRON POWDER DATA FOR $Li_{0.86}RuO_2$ WITH VALUES BASED UPON AN IDEAL NiAs-TYPE STRUCTURE

		$Li_{0.86}RuO_2$	Ideal NiAs
Ru	*X*	0.0	0.0
	Y	0.0	0.0
	Z	0.0	0.0
O	*X*	0.2501(26)	0.250
	Y	0.3316(35)	0.333
	Z	0.0	0.0
Li	*X*	0.0	0.0
	Y	0.5	0.5
	Z	0.5	0.5

Conclusions

Both lithium insertion systems Li_xRuO_2 and Li_xIrO_2 are two phase for $0 < x \gtrsim 0.9$, consisting of mixtures of the host rutile phase $x \approx 0$ and a limiting composition x = 0.9. $Li_{0.9}RuO_2$ and $Li_{0.9}IrO_2$ have orthorhombic cells with probable space group *Pnnm*. The structure of $Li_{0.9}RuO_2$ was solved from X-ray and neutron powder diffraction data. Features of the structure are a highly regular octahedral coordination for Li, a shorter Ru–Ru distance than in the host RuO_2 by 11%, and a very short Li–Ru distance. $Li_{0.9}RuO_2$ can be described as an ordered NiAs type structure closely related to $LiMoO_2$.

Acknowledgments

We thank J. Couper, J. D. Garrett, and H. F. Gibbs for technical assistance. Direct support for the MNR and an operating grant to J. E. Greedan were provided by NSERC.

References

1. D. W. MURPHY, F. J. DISALVO, J. N. CARIDES, AND J. V. WASZCZAK, *Mater. Res. Bull.* **13**, 1395 (1978).

2. W. H. BAUR, *Mater. Res. Bull.* **16,** 339 (1981).
3. D. E. COX, R. J. CAVA, D. B. MCWHAN, AND D. W. MURPHY, *J. Phys. Chem. Solids* **43,** 657 (1982).
4. D. B. ROGERS, S. R. BUTLER, AND R. D. SHANNON, *Inorg. Synth.* **13,** 135 (1971).
5. M. B. DINES, *Mater. Res. Bull.* **10,** 287 (1975).
6. R. D. SHANNON, *Acta Crystallogr. Sect. A* **32,** 751 (1976).
7. J. W. VISSER, *J. Appl. Crystallogr.* **2,** 89 (1969).
8. H. M. RIETVELD, *J. Appl. Crystallogr.* **2,** 65 (1969).
9. C. E. BOWMAN, *Acta. Chem. Scand.* **24,** 116 (1970).
10. W. C. HAMILTON, *Acta Crystallogr.* **18,** 502 (1965).
11. S. C. ABRAHAMS, J. M. REDDY, AND J. L. BERNSTEIN, *J. Phys. Chem. Solids* **27,** 997 (1966).
12. R. J. CAVA, A. SANTORO, D. W. MURPHY, S. ZAHURAK, AND R. S. ROTH, *J. Solid State Chem.* **42,** 251 (1982).
13. H. VOLLENKLE AND A. WITTMAN, *Z. Kristallogr.* **128,** 66 (1969).
14. A. F. WELLS, "Structural Inorganic Chemistry," 3rd ed., Clarendon, Oxford (1962).
15. L. KOESTER, "Neutron Physics," Springer Tracts in Modern Physics, Vol. 80, Springer-Verlag, New York (1977).